

HENRY

Hydraulic Engineering Repository

Ein Service der Bundesanstalt für Wasserbau

Conference Paper, Published Version

Mahgoub, Mohamed; Hinkelmann, Reinhard

Simulation of Density-Driven Flow Using a Two-Dimensional Surface Water Model

Zur Verfügung gestellt in Kooperation mit/Provided in Cooperation with:
TELEMAC-MASCARET Core Group

Verfügbar unter/Available at: <https://hdl.handle.net/20.500.11970/104302>

Vorgeschlagene Zitierweise/Suggested citation:

Mahgoub, Mohamed; Hinkelmann, Reinhard (2012): Simulation of Density-Driven Flow Using a Two-Dimensional Surface Water Model. In: Bourban, Sébastien; Durand, Noémie; Hervouet, Jean-Michel (Hg.): Proceedings of the XIXth TELEMAC-MASCARET User Conference 2012, 18 to 19 October 2012, St Hugh's College, Oxford. Oxfordshire: HR Wallingford. S. 173-178.

Standardnutzungsbedingungen/Terms of Use:

Die Dokumente in HENRY stehen unter der Creative Commons Lizenz CC BY 4.0, sofern keine abweichenden Nutzungsbedingungen getroffen wurden. Damit ist sowohl die kommerzielle Nutzung als auch das Teilen, die Weiterbearbeitung und Speicherung erlaubt. Das Verwenden und das Bearbeiten stehen unter der Bedingung der Namensnennung. Im Einzelfall kann eine restriktivere Lizenz gelten; dann gelten abweichend von den obigen Nutzungsbedingungen die in der dort genannten Lizenz gewährten Nutzungsrechte.

Documents in HENRY are made available under the Creative Commons License CC BY 4.0, if no other license is applicable. Under CC BY 4.0 commercial use and sharing, remixing, transforming, and building upon the material of the work is permitted. In some cases a different, more restrictive license may apply; if applicable the terms of the restrictive license will be binding.



Simulation of Density-Driven Flow Using a Two-Dimensional Surface Water Model

Mohamed Mahgoub, Reinhard Hinkelmann
 Chair of Water Resources Management and Modeling of Hydrosystems
 Technische Universität Berlin
 Berlin, Germany
mohamed.mahgoub@wahyd.tu-berlin.de

Abstract— To understand and quantify the effect of horizontal density variation on the behaviour of two-dimensional (2D) models, three test cases were investigated, two theoretical cases of a rectangular channel and a trapezoidal channel and the third is a real case of the Nile estuary at Rosetta close to the Mediterranean Sea. Having the ability to include the spatial variation of density, TELEMAC-2D modelling system which solves 2D (depth averaged) Saint-Venant equations was used for this purpose.

For these three cases, three scenarios were simulated in stagnant and flowing water: horizontal density variation only, diffusion only and both density variation and diffusion together. The three scenarios were considered in case of stagnant water for the two theoretical cases; the simulations in flowing water are then closer to the real conditions of the Nile.

The results show that the impact for the density variation is higher than that of diffusion. The results further show that the shape of the cross section (rectangular or trapezoidal) has a considerable influence on the results which was not expected. It can be concluded that the effect of horizontal density variation should be taken into account in 2D simulations of the Nile or other tideless estuaries.

I. INTRODUCTION

The anticipated sea level rise due to climate change could have great impact on estuaries and river mouths. The balance status that is present currently between fresh water and saline water in river mouths could change. Such phenomenon has to be considered in modelling of surface water at estuaries [9]. Meanwhile, estuaries are characterised by the presence of density-driven flow, where the variation of density due to salinity difference forces the saltwater landward. In a tideless sea, as the case of the Mediterranean Sea, the estuary is characterised by strong stratification and saltwater intrusion into the river system. The saltwater layer underlies the freshwater layer of the river [4].

The stratification effect cannot be modelled in a 2D model, because the concentration is averaged over the depth. Nevertheless, the effect of spatial density variation (in the horizontal direction) as a function of salinity concentration can be considered in a 2D model leading to a barotropic and baroclinic pressure gradient (Fig. 1).

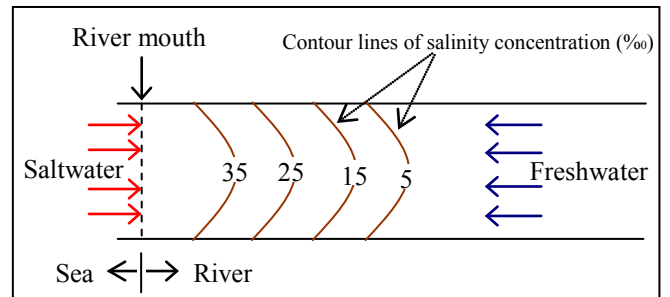


Figure 1. Schematic plan for the spatial variation of salinity at an estuary.

Therefore, the aim of this research is to understand and quantify the effect of horizontal density variation using the method presented in [5] which is detailed hereafter and is embedded in the code of the TELEMAC-2D modelling system used in this research for modelling three test cases including one real case for the Nile River estuary.

II. GOVERNING EQUATIONS

A. Saint-Venant equations

The main governing equations in 2D surface water flow are 2D Saint-Venant equations which have been derived with averaging over the vertical. The equations in their non-conservative form can be written as follows:

Continuity equation

$$\frac{\partial h}{\partial t} + \vec{u} \cdot \overrightarrow{\text{grad}}(h) + h \cdot \text{div} \vec{u} = S_{ce} \quad (1)$$

Momentum equations

$$\frac{\partial u}{\partial t} + u \frac{\partial u}{\partial x} + v \frac{\partial u}{\partial y} = -g \frac{\partial Z_s}{\partial x} + F_x + \frac{1}{h} \text{div}(h v_e \overrightarrow{\text{grad}} u) \quad (2)$$

$$\frac{\partial v}{\partial t} + u \frac{\partial v}{\partial x} + v \frac{\partial v}{\partial y} = -g \frac{\partial Z_s}{\partial y} + F_y + \frac{1}{h} \text{div}(h v_e \overrightarrow{\text{grad}} v) \quad (3)$$

h is the water depth, u and v are the velocity components, Z_s is the surface elevation, ν_e is the diffusion (molecular turbulent and viscosity), g is the gravitational acceleration, S_{ce} is source or sink of the flow, and F_x and F_y are source or sink terms for momentum; in this case the buoyancy forces due to spatial variation in density (detailed in section B.) and the terms due to bottom friction. The latter can be expressed according to Manning law as follows:

$$F_x^f = -\frac{u}{\cos \alpha} \frac{gn^2}{h^{4/3}} \sqrt{u^2 + v^2} \quad (4)$$

$$F_y^f = -\frac{v}{\cos \alpha} \frac{gn^2}{h^{4/3}} \sqrt{u^2 + v^2} \quad (5)$$

where n is Manning coefficient, α is the angle of bottom slope.

B. Spatial variation of density

The aforementioned equations (1, 2 and 3), as averaged over the vertical, cannot represent the stratification resulting from the vertical variations of density, itself a function of salinity or of the temperature [5].

However, it is possible to consider the horizontal variations in density by the method presented in [5]. If S is the salinity and θ is the temperature, water density (ρ) will be a function $\rho(S, \theta)$, where S and θ are variable in space and time. These variations cause two effects which are dilatation of water and differential effects of gravity [5].

The dilatation of water is a secondary effect which can be ignored. The differential effect of gravity due to variations in salinity is very important especially in estuaries, therefore it should be considered. Hervouet [5] used Boussinesq's hypothesis which accounts for the variations in salinity only in terms of gravity.

According to [6], the buoyancy terms in Saint-Venant equations can be integrated from those of Navier-Stokes equation as follows:

$$-\frac{1}{\rho_0} \overrightarrow{\text{grad}}[\rho g(Z_s - z)] \quad (6)$$

Z is the elevation of the bottom. Integrating this term between the bottom and the surface while considering the spatial variations of the density will produce two terms which are in the non-conservative form [6]:

- Barotropic pressure gradient: $-\frac{\rho}{\rho_0} \overrightarrow{g} \overrightarrow{\text{grad}} Z_s$,

this term will replace the term $\overrightarrow{g} \overrightarrow{\text{grad}} Z_s$ in equations (2) and (3).

- Baroclinic pressure gradient: $-\frac{g}{\rho_0} \frac{h}{2} \overrightarrow{\text{grad}} \rho$, this term will be added to the bottom friction (4 and 5) to give F_x and F_y in equations (2) and (3).

The density is calculated from the following equation:

$$\rho = \rho_{ref} \left[1 - (7(\theta - \theta_{ref})^2 - 750S)10^{-6} \right] \quad (7)$$

θ_{ref} denotes the reference temperature of 4°C and ρ_{ref} is the reference density at zero salinity (equals to 999.72 kg/m³).

C. Transport equation

The transport equation in its non-conservative form in 2D can be written as follows:

$$\frac{\partial T}{\partial t} + \overrightarrow{u} \overrightarrow{\text{grad}} T - \frac{1}{h} \text{div}(\nu_i \overrightarrow{\text{grad}} T) = \frac{(T_{sce} - T)S_{ce}}{h} \quad (8)$$

T is the tracer concentration, T_{sce} is the source value of the tracer and ν_i is the diffusion coefficient (molecular and turbulent diffusion).

III. MODELLING SYSTEM

TELEMAC-2D modelling system has been chosen to set up a 2D numerical model for the test cases. TELEMAC-2D simulates open channel flow using Finite Element Method (FEM) for solving the two-dimensional Saint-Venant equations. TELEMAC-2D can consider the transport of a passive tracer. The primary variables are the water depth the velocity and the concentration of tracer averaged over the vertical [7]. The abovementioned equations for spatial variation of density are embedded in TELEMAC-2D, so it is suitable for the purpose of this research.

TELEMAC-2D allows the choice among several laws of friction, turbulence models, stabilisation methods and solvers. In this research the narrow (N) distributive scheme was used for the hydrodynamic and transport modelling. The solver applied in the research is the Generalised Minimum RESidual method (GMRES) for the non-symmetric matrices [11]. TELEMAC-2D generally uses linear triangular finite elements, but it can also work with quadrilateral elements.

TELEMAC-2D has been applied for numerous studies in fluvial and maritime hydraulics [1, 9 and 11]. The modelling process with TELEMAC-2D consists of pre-processing with MATISSE, processing and post-processing with RUBENS.

IV. TEST CASES

Three test cases were analysed in this research, two of them are theoretical cases of a rectangular channel and a trapezoidal channel and the third is a real case of the Nile estuary at Rosetta. For the two theoretical cases, four scenarios were modelled. These are:

1. Stagnant water with horizontal density variation only and ignoring diffusion
2. Stagnant water with diffusion only and ignoring horizontal density variation
3. Stagnant water with both diffusion and horizontal density variation
4. Flowing water with both diffusion and horizontal density variation

The aim of the previous scenarios was to check how the horizontal variation of density can affect the results and to compare its impact with the one of diffusion. In addition, the shape impact was also analysed. The simulations in flowing water are then closer to the real conditions of the Nile, so the scenarios 1, 2 and 3 were also modelled in this case but in flowing water instead of stagnant water.

A. Rectangular channel

The channel dimensions are 5 m, 200 m and 1000 m for the depth, the width and the length respectively, and with zero bottom slope. A triangular grid of 10 m discretisation length was generated by MATISSE; the grid was refined in the middle part of the channel where a 4 m discretisation length was used due to the choice of the initial conditions (see Fig. 3). The total number of nodes is 3303 and the total number of elements is 6344 (Fig. 2).

The channel has two open boundaries which are the upstream (U.S.) boundary, where the flow is given (zero in case of stagnant water and 80 m³/s in case of flowing water) and zero salinity, and the downstream (D.S.) boundary where

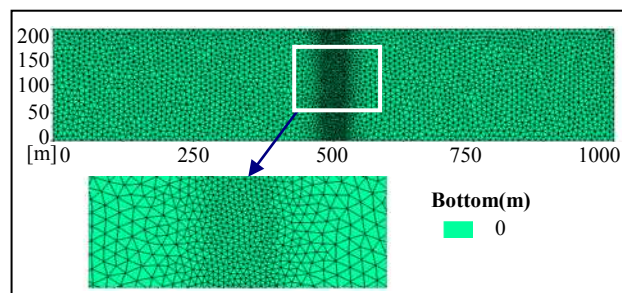


Figure 2. Grid of the rectangular channel.

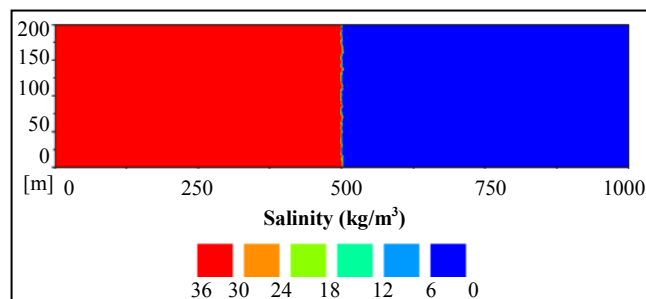


Figure 3. Initial conditions for salinity transport.

a water level of 5 m and a salinity concentration of 35 mg/l are imposed. Manning friction coefficient, similar to that of the Nile case, of 0.022 was employed here. The time step of the simulation was 5 seconds.

The initial condition for salinity was that half of the channel (starting from the D.S. boundary) was saline water and the other half was fresh water as shown in Fig. 3. The viscosity coefficient (molecular and turbulent) was assumed to be 0.001 m²/s.

The simulation of the rectangular channel showed smaller impact for the diffusion than of density variation as shown in Fig. 4A and 4B for 100 days of simulation time. For longer simulation time the impact of density variation will be much bigger as it still shows slow change while for the case of diffusion no further change was noticed after 10 days of simulation.

As the impact in case of turbulent diffusion only was quite small, combining both diffusion and density variation showed very similar results as the case of density variation only (Fig. 4C).

When introducing a flow from the U.S. boundary (80 m³/s), the saline water moved towards the D.S. boundary (Fig. 4D) very quickly (Fig. 4D shows the result after about 80 minutes only) due to the momentum produced from the flow velocity which is higher than the one due to the spatial variation of density. No doubt that changing the discharge will impact on the movement speed of the saline water.

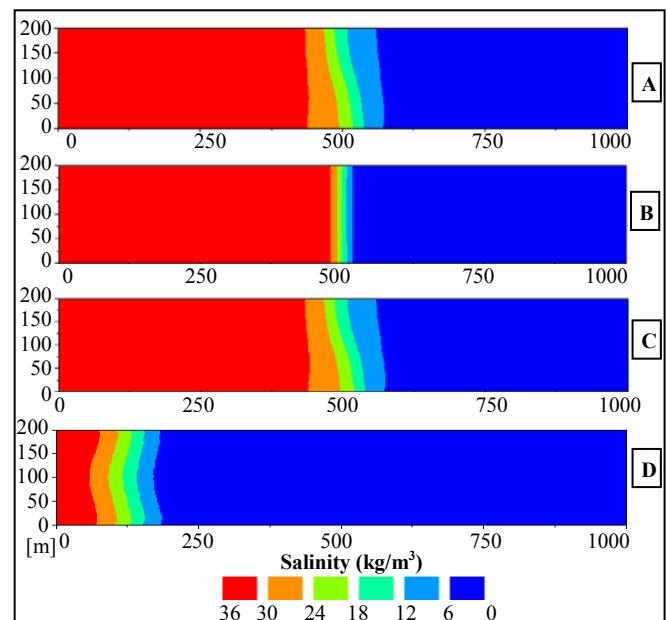


Figure 4. Salinity transport for the rectangular channel for A) stagnant water with horizontal density variation only, B) stagnant water with diffusion only, C) stagnant water with horizontal density variation and diffusion and D) flowing water with horizontal density variation and diffusion.

B. Trapezoidal channel

The channel has a total length of 1000 m; the cross section is shown in Fig. 5. The grid configurations, the boundary conditions and the numerical parameters are the same as in the previous case. The total number of nodes is 3325 and the total number of elements is 6388 (Fig. 6). The same initial condition shown in Fig. 3 is used in this case also.

The changes are faster in this case than in the case of the rectangular channel. After 10 days of simulation, an obvious difference can be noticed between the four modelled scenarios. In the case of horizontal density variation only, most of the channel is turned to be saline water, which means that the impact of the salinity difference forced the fresh water to leave the system (Fig. 7A).

Changes in the salinity concentration with respect to the depth variation are also noticed, where higher concentrations are in the deeper parts, this is consistent with the results of [3] where it was concluded that lateral variations of the depth cause a lateral variation of the turbulence and bottom friction which results in a tilt of the gravitational flow responsible for the density driven flow in 2D model. In addition, the horizontal pressure force due to horizontal density gradient is proportional to the depth; therefore the tendency of the heavier salty water to replace the lighter fresh water landward is stronger when increasing the depth [2].

The impact of turbulent diffusion was much smaller than the impact of density variation; it is limited in a small part in the middle of the channel (Fig. 7B). The influence of turbulent diffusion was quite similar in both the trapezoidal channel and the rectangular channel (Figs. 4B and 7B) which is not the case in the density variation impact.

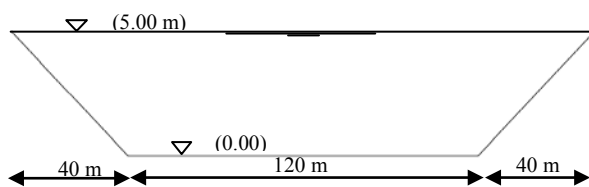


Figure 5. Cross section of the trapezoidal channel.

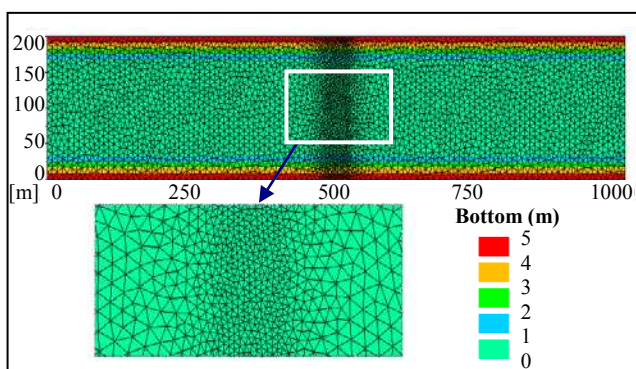


Figure 6. Grid of the trapezoidal channel.

When combining diffusion and density variation together (Fig. 7C), only a slight difference from the case of the density variation only can be seen; instead of the uniform variation with respect to the horizontal axes, the variation of salinity was only in the lower part of the channel.

Like the case of the rectangular channel mentioned earlier, introducing a slow flow to the system (80 m³/s) caused that the saltwater moves towards the D.S. boundary (Fig. 7D). However the shape of the saltwater wedge is completely different from the case of the rectangular channel. That also emphasises the shape impact on the transport of salinity.

C. River Nile estuary

The last controlled reach of Rosetta branch of the Nile River (Fig. 8) is chosen to be compared to the theoretical cases. The reach under study is located between 31.32° and 31.45° north and 30.34° and 30.53° east with a total length of about 35 km. Edfina Barrage controls the flow in the reach under study at U.S. side, and it ends with the Mediterranean Sea at D.S. side.

The water depth ranges from 2.30 m to about 26.5 m. The average width of the domain is about 500 m. The average discharge during the year is 83.6 m³/s and the average water level at D.S. is 0.37 m above mean sea level (+msl). The average discharge at the U.S. side and average sea level at D.S. side were used for the simulation.

A triangular grid is generated with MATISSE. The discretisation length of the elements is 40 m in parts of the domain, and in specific parts where the bottom level has a sharp slope and in the parts of small width a finer grid with

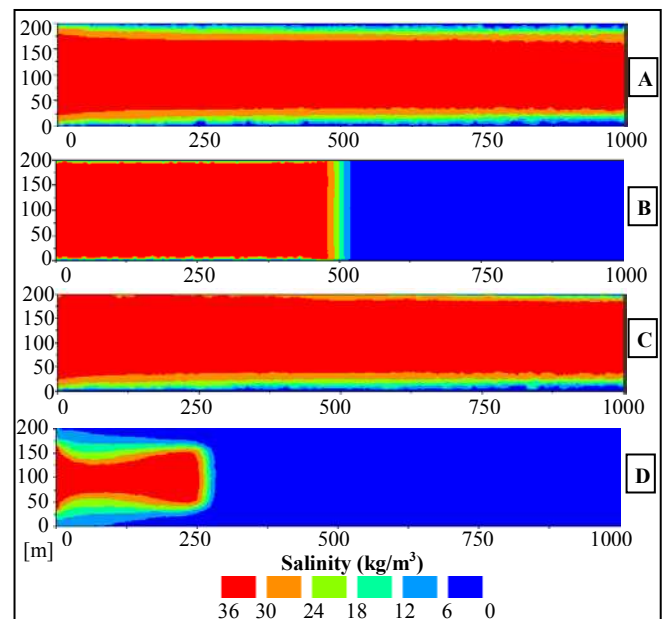


Figure 7. Salinity transport for the trapezoidal channel for A) stagnant water with horizontal density variation only, B) stagnant water with diffusion only, C) stagnant water with horizontal density variation and diffusion and D) flowing water with horizontal density variation and diffusion.



Figure 8. Map of the reach under study.

20 m discretisation length is generated. The total number of nodes is 19448 and the total number of elements is 36669 (Fig. 9).

The model is bounded from its U.S. side by Edfina Barrage where the discharge is known and from the D.S. side with the Mediterranean Sea where the water level is known, so those are considered the only two open boundaries in the domain and all the other boundaries, mainly the banks, are closed.

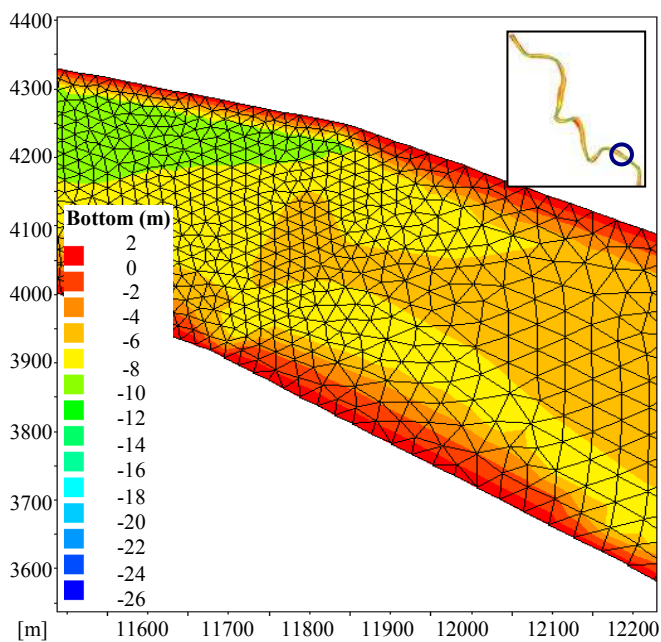


Figure 9. Grid at one position for Nile estuary case.

The simulation was carried out with a time step of 5 seconds. A total simulation time of three days was carried out to reach a steady state condition assuming an initial condition of zero velocity and initial water level of 0.37 m+msl. This steady state case was later employed as initial condition for the transport simulation. Manning friction coefficient of 0.022 [7] and a simple turbulence model with constant viscosity ($\nu = 0.01 \text{ m}^2/\text{s}$) being equal to the turbulent diffusion were chosen. The initial condition for salinity concentration was calculated based on the following equation [9]:

$$L_i = \frac{2h_0}{0.5R_e^{-0.25}} \left(\frac{1}{2Fr_{do}^2} - 2 + 3Fr_{do}^{2/3} - \frac{6}{5}Fr_{do}^{4/3} \right) \quad (9)$$

L_i is the intrusion length of the saline water inside the river, R_e is the Reynolds number which is expressed as $4R_h u_0 / \nu$, Fr_{do} is the densimetric Froude number which expressed as $u_0 / \sqrt{g\Delta\rho h_0 / \rho}$, h_0 is the water depth at the river mouth, R_h is the hydraulic radius, u_0 is the velocity of river flow at the mouth, ρ is the fresh water density, $\Delta\rho$ is the density difference between saltwater and fresh water and g is the gravitational acceleration. Equation (9) was used to calculate the total length of saltwater intrusion inside the river considering the D.S. boundary with a salinity concentration of 38.5 kg/m^3 , the intrusion length was found to be 15329 m. Then a linear change of the concentration was assumed, so the initial condition of salt concentration was set to be as shown in Fig. 10.

Comparing the results after one day of simulation time for the case of horizontal density variation only to the case of turbulent diffusion only (Figs. 11A and 11B) showed that the intrusion length was rapidly decreased in both cases (if

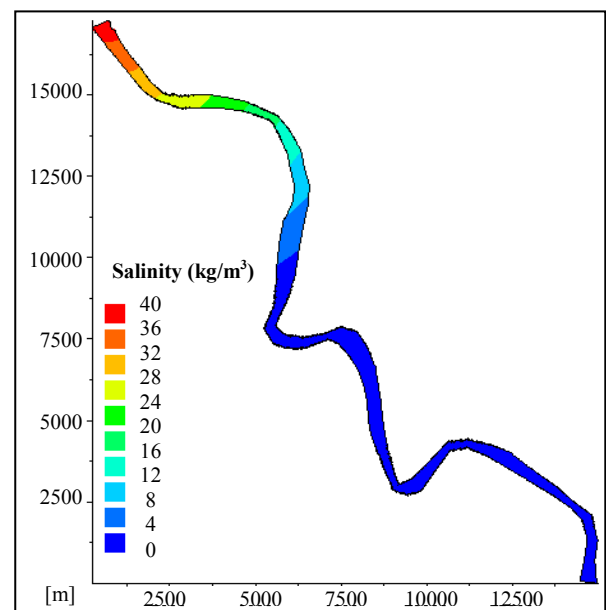


Figure 10. Initial conditions of salt concentration.

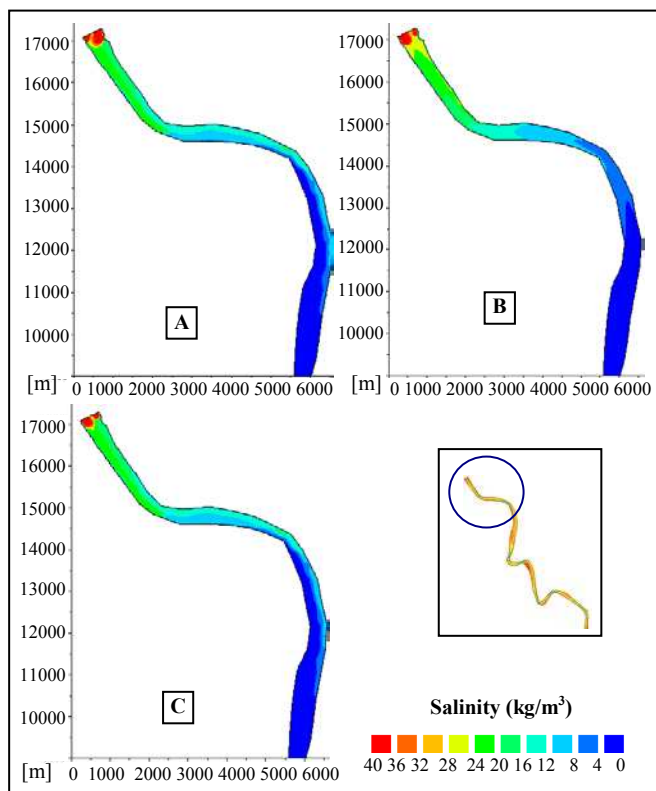


Figure 11. Salt concentration after one day of simulation time for the Nile estuary for: A) horizontal density variation only, B) turbulent diffusion only and C) horizontal density variation and turbulent diffusion.

compared to the initial conditions), however it was less in the case of the turbulent diffusion only. So, the impact of density variation is quite higher than the turbulent diffusion as it causes more momentum, therefore it has higher tendency to resist the momentum of the flow.

For the case of both turbulent diffusion and horizontal variation of density together (Fig. 11C) the results seem to be similar to the one of horizontal variation of density only (Fig. 11A). The results of the Nile case is the same result found in the two theoretical cases described earlier (higher impact for horizontal variation of density than diffusion). However, the results differ much from the initial condition of salinity concentration, which could be because the 1D nature of the equation used for calculating the initial condition.

V. CONCLUSIONS

TELEMAC-2D modelling system was used in this research to understand and quantify the impact of the spatial variation of density in a 2D model with the aid of the method presented in [5]. In addition, the impacts of diffusion and density variation on the flow were compared.

The simulation of the all the case studies revealed that the impact of density variation is higher than the turbulent diffusion. The shape influenced the results, where much

faster change is noticed in the trapezoidal channel (approximately the whole domain turned to be saltwater in 10 days simulation time), while the change was quite slow in the rectangular channel. However, the impact of the shape was recorded only for the case of horizontal variation of density and it was not observed for the case of diffusion, thereof the diffusion is independent of the shape. The effect of the water depth was also noticed; higher salt concentration was combined with higher water depth (as described in the case of trapezoidal channel).

For the Nile case study, smaller saltwater intrusion length was also noticed for the case of diffusion only compared to the case of horizontal variation of density for the same simulation conditions, which could be related to the higher momentum caused by the horizontal variation of density. This result confirms the previous ones.

Through this research, it was proved that 2D models can be employed to simulate horizontal density-driven flow and TELEMAC-2D modelling system is suitable for this purpose. In addition, this research emphasises the importance of including the spatial variation of density when simulating tideless estuaries as in the case of the Nile River.

REFERENCES

- [1] A. Jourieh, M. Heintz, R. Hinkelmann and M. Barjenbruch, "Simulation of Combined Sewer Overflows Spreading in a Slowly Flowing Urban River", 33rd IAHR Congress: Water Engineering for a Sustainable Environment, Vancouver, British Columbia, Canada, ISBN: 978-90-78046-08-0, 2009.
- [2] C. Li and A. Valle-Levinson, "Separating baroclinic flow from tidally induced flow in estuaries", *Journal of Geophysical Research*, vol. 103, No. C5, 405-10,417, 1998.
- [3] D. V. Hansen and M. Rattray, "Gravitational circulation in straits and estuaries", *Journal of Marine Research*, vol. 23, pp. 104-22, 1965.
- [4] H. Chanson, "Environmental hydraulics of open channel flows", Elsevier Butterworth-Heinemann Linacre House, ISBN: 0750661658, 2004.
- [5] J. M. Hervouet, "Hydrodynamics of Free Surface Flows, modelling with the finite element method", John Wiley and Sons Ltd., England, ISBN 978-0-470-03558-0, 2007.
- [6] LNHE, National Hydraulics and Environment Laboratory, "telemac2d concept note", http://www.opentelemac.org/downloads/MANUALS/TELEMAC2D/prin30_gb.pdf, 2010.
- [7] LNHE, National Hydraulics and Environment Laboratory, "telemac2d user manual", http://www.opentelemac.org/downloads/MANUALS/TELEMAC2D/telemac2d_user_manual_v6p0.pdf, 2010.
- [8] M. K. Mahmoud, A. El-Balasy and E. A. El-Ghorab, "Mathematical model of the sedimentation problem at Rosetta promontory", Tenth International Water Technology Conference, IWTC10, Alexandria, Egypt, 2006.
- [9] M. Mahgoub, A. Jourieh and R. Hinkelmann, "Two-dimensional flow and transport simulation of the Nile estuary investigating impacts of sea level rise", 2nd IAHR Europe Congress, Munich, Germany, June 2012.
- [10] M. Markofsky, "Strömungsmechanische Aspekte der Wasserqualität", Oldenbourg Verlag, München, Deutschland, 1980.
- [11] R. Hinkelmann, "Efficient Numerical Methods and Information-Processing Techniques for Modeling Hydro- und Environmental Systems", *Lecture Notes in Applied and Computational Mechanics*, vol. 21, Springer-Verlag, Berlin, Heidelberg, 2005.